GEOL 1008 1995

Pergamon

Journal of Structural Geology, Vol. 17, No. 12, pp. 1725 to 1740, 1995

0191-8141/95 $9.50+0.00

0191-8141(95)00066-6

Compressional and extensional tectonics in an arc system: example of the Southern Apennines

J.-C. HIPPOLYTE, J. ANGELIER and E. BARRIER

Département de Géotectonique (URA 1759 du CNRS), Université P. et M. Curie, Boîte 129, 75252 Paris Cedex 05, France

(*Received* 28 *October* 1994; *accepted in revised form* 1 *June* 1995)

Abstract—Adopting the Southern Apennines as a case example, we determine the relationships between extensional and compressional structures within an arc system, based on tectonic analysis in the field. We show that, in addition to the well-known occurrence of inner extensional structures during frontal accretion, two other types of extensional structures are present in the Southern Apennines. We classify the three types of extensional structures depending on their chronologies with the accretion of the thrust unit, and we characterize them in terms of palaeostresses.

Some normal faults of the mountain chain are old extensional structures formed in a foreland basin. In the Matese Mountains, such faults with offsets ranging several hundred metres are sealed by a late Neogene thrust sheet. These foredeep structures were created by extension trending almost perpendicular to the axis of the present-day foreland basin.

Other normal faults, located closer to the Tyrrhenian sea, developed simultaneously with the Pliocene–Quaternary accretion of thrust sheets at the front of the belt. In the Salerne graben (a Tyrrhenian Basin structure), extension occurred perpendicular to the compression that prevailed at the front of the mountain belt. A stress gradient existed between the outer part of the arc (with σ_1 trending ENE–WSW) and the inner part (with σ_2 trending ENE–WSW).

In the Southern Apennines, middle Pleistocene–Holocene normal faults post-date all compression and thrusting. The corresponding recent stress field (NE–SW extension) results from uplift of the previously subsiding Adriatic lithosphere.

We conclude that a given thrust unit of this NW–SE-trending mountain chain may have successively undergone NE–SW extension in the foreland basin, NE–SW compression during the accretion, NW–SE extension in the back-arc region and NE–SW extension during the recent evolution of the prism. The succession of these tectonic regimes has induced complex structures, as commonly observed in an arc system.

INTRODUCTION

Understanding the mechanism that allows co-existence of compression in an accretionary prism and extension in a back-arc basin is a major issue in the study of arc systems. In the Western Mediterranean, the Tyrrhenian arc (Apennines, Calabria and Sicilia) and its back-arc basin (Fig. 1a) show the juxtaposition of these two distinct modes of deformation. Extensional and compressional tectonics were active during the same period, simultaneous with the Neogene rollback of the sinking Ionian lithosphere (Moussat 1983, Malinverno & Ryan 1986). Most of the Apennines mountain belt results from late Miocene–Quaternary compression (Casero *et al.* 1988, Patacca *et al.* 1990). At the same time, extension produced the Tyrrhenian oceanic Basin partly superimposed on the eo-Alpine chain (Haccard *et al.* 1972, Scandone 1979). The Tyrrhenian Basin is in a back-arc position with respect to the late Miocene–Quaternary chain. It is composed of two sub-basins (Fig. 1a): the Vavilov sub-basin opened in the western part of the present Tyrrhenian sea during late Miocene and Pliocene, whereas, to the southeast, the Marsili sub-basin opened during Pliocene–Quaternary (Finetti & Del Ben 1986, Sartori 1989, Kasten *et al.* 1990).

Structural analyses onshore in the Tyrrhenian arc allow determination of the relationships between these two contrasting tectonic processes. It was shown that compressional and extensional structures (Fig. 1b) are superimposed in various ways. However, their genetic relationships are often obscure. Since most extensional structures post-date compression (e.g. Boccaletti *et al.* 1983), the presence of extension in the mountain chain is usually interpreted as the result of the eastward migration of the Tyrrhenian extensional area (e.g. Boccaletti *et al.* 1983, Malinverno & Ryan 1986, Bartole *et al.* 1984, Doglioni 1991, Fusi & Garduno 1992, Oldow *et al.* 1993). On the other hand, inversion of extensional structures may be related to block rotations (Knott & Turco 1991). More complex chronological relationships between extensional and compressional structures may also result from alternating periods of compression and extension in the same area (e.g. Gars 1983, Auroux 1984, Boccaletti *et al.* 1984, Bernini *et al.* 1990).

In this paper, we address the problem of space and time distribution of tectonic forces in terms of stresses. Our approach is based on measurements of fault slip orientations. We use the stress inversion techniques (Angelier 1989) to relate the observed structures to their causative tectonic forces. Favourable conditions for such a study were found in the Southern Apennines (Fig. 1b). The chronology of structures and stresses is established based on successions of tectonic movements and

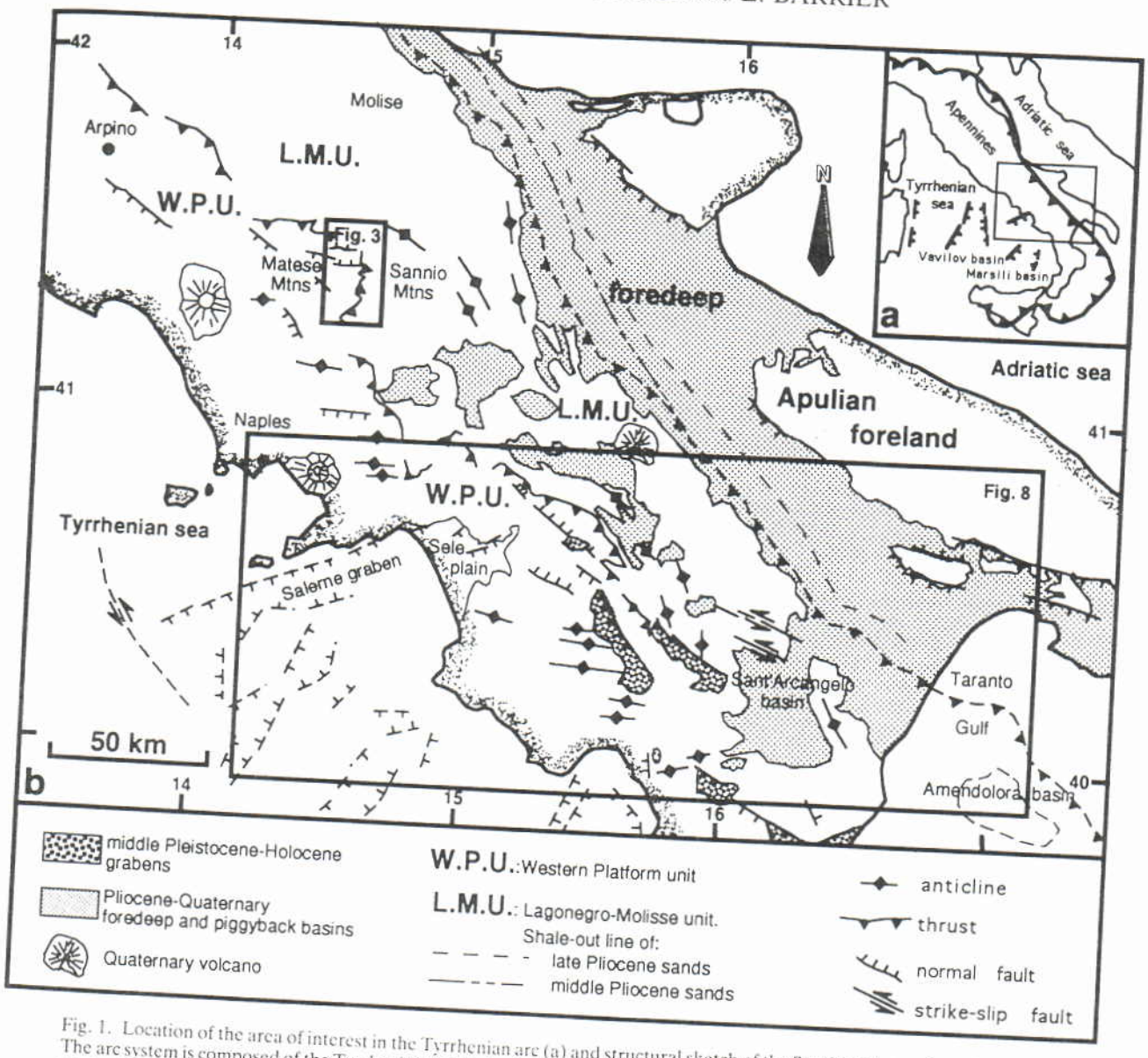

Fig. 1. Location of the area of interest in the Tyrrhenian arc (a) and structural sketch of the Southern Apennines, Italy (b). The arc system is composed of the Tyrrhenian arc, its foreland basin and its back-arc basin including the Vavilov and Marsili sub-basins. Note in (b) the mixture of compressional and extensional structures in the mountain belt. The shale-out lines, from Casero *et al.* (1991) show the progressive foredeep sediments onlap on the carbonates of the Apulian foreland, as well as the major advance of the thrust front in the southern area. The frontal thrust is buried under middle Pleistocene–Recent sediments.

stratigraphic dating, including the identification of syntectonic marine sediments of various ages. Combined palaeostress determinations and structural analyses enable us to determine the age, origin and significance in the history of the arc of the observed extensional and compressional structures.

GEOLOGICAL FRAMEWORK

The Southern Apennine is considered an accretionary wedge (Pescatore & Slaczka 1984, Roure *et al.* 1991). It results mainly from NE-vergent thrusting of Mesozoic–Tertiary sedimentary units over the Apulian foreland (Figs. 1b and 2). According to the most recent models (Mostardini & Merlini 1988, Casero *et al.* 1988), the eastern thrust units (Lagonegro–Molise) derive from a relatively deep Mesozoic–Tertiary basinal domain originally located between two shallow-water carbonate platforms. Thrust units deriving from a western platform crop out in the western (Tyrrhenian) side of the belt (Figs. 1b and 2). Other units deriving from an eastern platform (Apulian platform) constitute a deeply buried overthrust belt detected by seismic data (Fig. 2).

A widely accepted model for the formation of an accretionary wedge is that thrusting and foredeep subsidence have progressively migrated towards the foreland. The Neogene cratonward shifting of the Apennine foredeep is well documented (Bortolotti *et al.* 1970, Casnedi *et al.* 1982, Ricchi Lucchi 1986). In the Southern Apennines, because of the progressive flexure of the Adriatic plate, the Pliocene–Quaternary terrigeneous marine deposits of the foredeep basin overlap Mesozoic–Tertiary shallow-water carbonates of the eastern platform (Fig. 2). Near the Tyrrhenian coast, the presence of Messinian clastic sediments above the car-

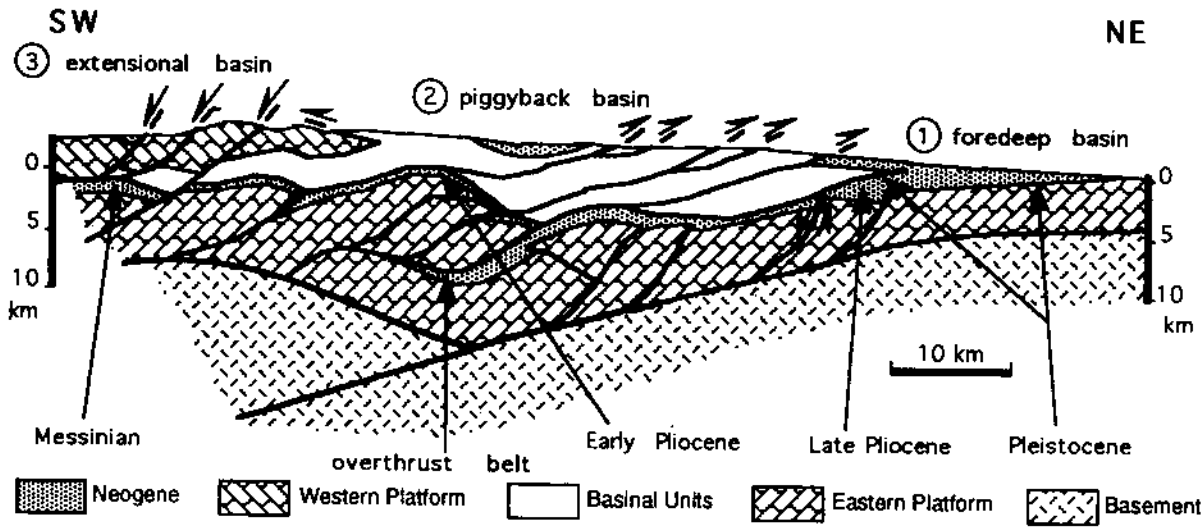

Fig. 2. Schematic cross-section of Southern Apennines (modified from Casero *et al.* 1991) showing the relationship between structural units and syn-tectonic basins (foredeep, piggyback and back-arc basins). The east–west variation in the age of the foredeep sediments shows the progressive age of the Eastern (Apulian) Platform subsidence.

bonates of the eastern platform and under the thrust sheets confirms the shifting of the subsidence (Casero *et al.* 1988) (Fig. 2).

The eastward migration of the deformation (Pescatore & Slaczka 1984) is also demonstrated by the analyses of syn-orogenic intramountain basins unconformably overlying the allochthonous units (Casero *et al.* 1988, Roure *et al.* 1991) and named piggyback basins (Ori and Friend, 1984) (Fig. 2). In particular, the ages of the Pliocene–Quaternary piggyback basins illustrate the progressive eastward shift of thrusting in the eastern platform units (Hippolyte *et al.* 1994b).

In this model of prograding deformation, supported by dating of compression in the belt and dating of flexure in the foreland, compression is considered to be the unique and permanent mode of deformation at the front of the belt. This consideration is supported by detailed palaeostress analyses in piggyback basins, showing that compression lasted for long periods and probably was even continuous on the eastern side of the belt (Hippolyte *et al.* 1994b). The extension that developed mainly on the Tyrrhenian side of the belt (Fig. 2) is hard to reconcile with this model (e.g. Ghisetti & Vezzani 1981, Moussat 1983, Malinverno & Ryan 1986, Roure *et al.* 1990). We have analysed the structure and faulting in various syn-orogenic basins to determine the place and significance of extension within the geodynamic process of accretion. In this paper, we show that extensional structures of very different ages are present on the Tyrrhenian side of the belt. The relationship with the compressional structures is determined. Three cases are observed: (1) extension pre-dating thrusting and compression; (2) extension on the Tyrrhenian side of the belt contemporaneous with thrusting and compression on the front of the belt; and (3) extension post-dating compression. These relationships are illustrated through several examples, where they are characterized in terms of stresses.

EXTENSION PRECEDING THRUSTING

The carbonate thrust units on the western side of the belt (W.P.U. in Fig. 1b) are deformed both by extensional and compressional tectonics. Extensional structures are particularly well developed in the Matese Mountains (Figs. 1b and 3), where normal faults with offsets of several hundred metres are common (Figs. 3 and 4a). Folds, reverse faults and strike-slip faults are also present (Clermonté & Pironon 1979). All these structures are related to several states of stress including three extensional ones and three compressional and strike-slip ones.

First of all, the nature, orientation, relative chronology and stratigraphic age of each state of stress need to be discussed. A NNE–SSW extension (state of stress A in Fig. 4a) gave the best expressed deformation, with E–W trending normal faults (Fig. 3) which have large offsets (Fig. 4a). We also determined two perpendicular extension trends, NE–SW and NW–SE (Table 1, states of stress B and C) but the corresponding normal faults have much smaller offsets. A pervasive N–S to NNE–SSW compression (state of stress D in Fig. 4a) induced folding and reverse faulting. Local strike-slip and reverse motions are due to ESE–WNW and ENE–WSW compressions (states of stress E and F, respectively, Table 1).

All these faults, normal, strike-slip or reverse, affect the whole stratigraphic sequence, including the most recent deposits of the Matese unit of late Miocene age (Fig. 4a). In order to establish the chronology of these structures, we paid particular attention to geometrical relationships. For instance, when several striations are present on a single fault plane, their order of succession reveals the chronology of the relative states of stress. In the western Matese Mountains, 32 unambiguous chronologies of slickenside superposition are found. Using the chronology matrix analysis proposed by Angelier

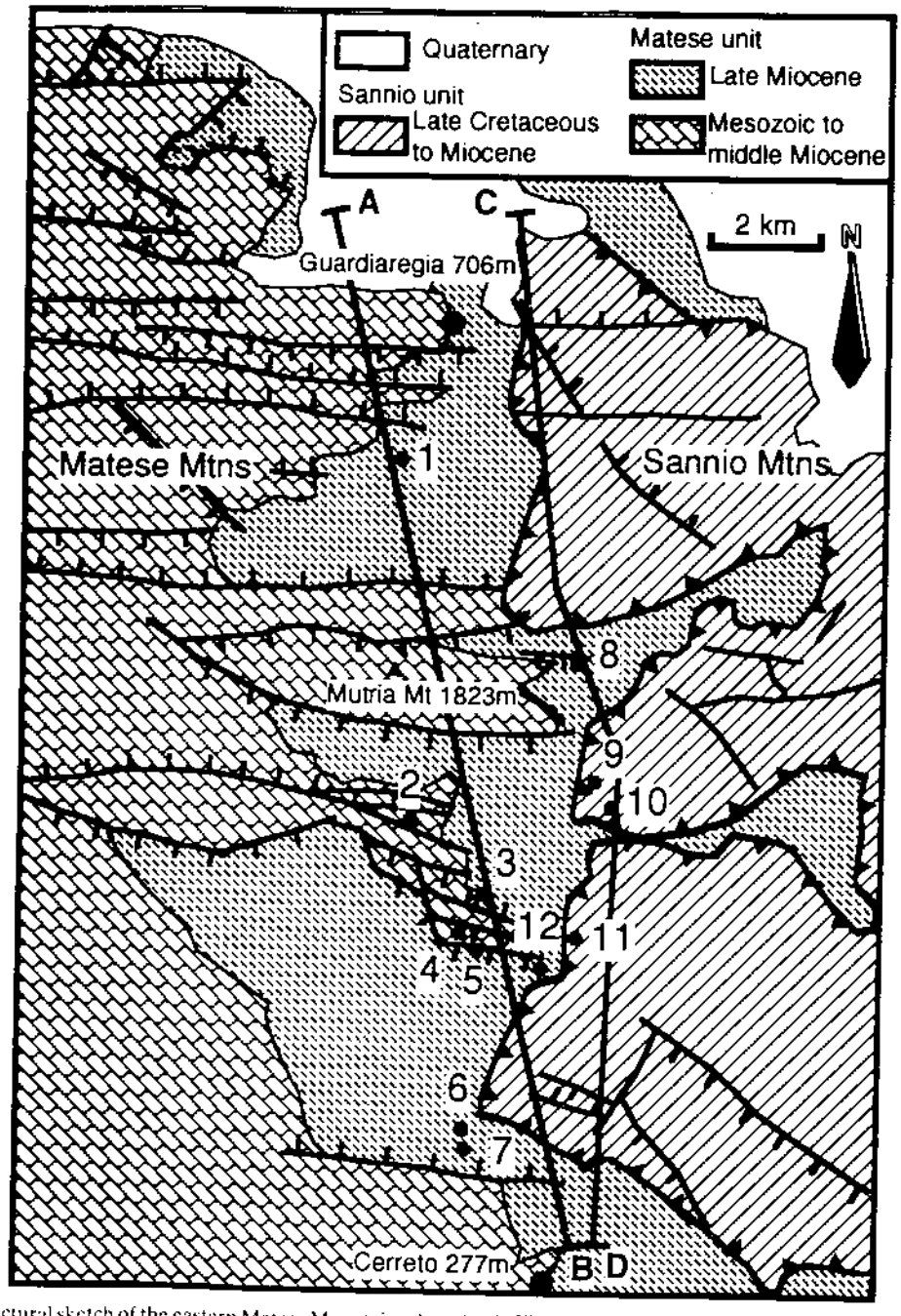

Fig. 3. Structural sketch of the eastern Matese Mountains (location in Fig. 1b). Note the differences of fracture orientations in the Sannio thrust unit and in the underlying Matese unit.

(1991), we determined the possible succession of states of stress. Among 720 possible chronologies for six states of stress, only three are consistent with all the relationships observed in the field (Fig. 5). Furthermore, for each of these three solutions, all extensional states of stress (states of stress A, B and C) pre-date compression. We conclude that, despite the apparent complexity of the palaeostress history, the widespread extensional tectonics of the Matese area certainly pre-dates the compressional tectonics.

Other criteria for chronology are found, such as cross-cutting relationships. For instance, in site 1 of Fig. 3, the normal faults of the NNE–SSW extension are offset by bedding plane faults related to folding under the NNE–SSW compression (Fig. 6a). Moreover, some of these normal faults underwent strike-slip to reverse reactivation due to the NNE–SSW compression. Both criteria indicate that normal faulting pre-dates compression. A common consequence of this chronology is that some normal faults, that have undergone tilting, now appear as nearly vertical faults or reverse faults (Figs. 4a, 6b & c).

This chronology between extension and compression is also recognized at the regional scale. The major structures of the Matese Mountains plunge to the east beneath the Sannio thrust unit (Figs. 3 and 7a) (Clermonté & Pironon 1979). The large E–W trending normal faults, which are a common feature in the Matese Mountains, do not exist in the overlying Sannio thrust sheet (Fig. 3). Furthermore, no mappable extension of

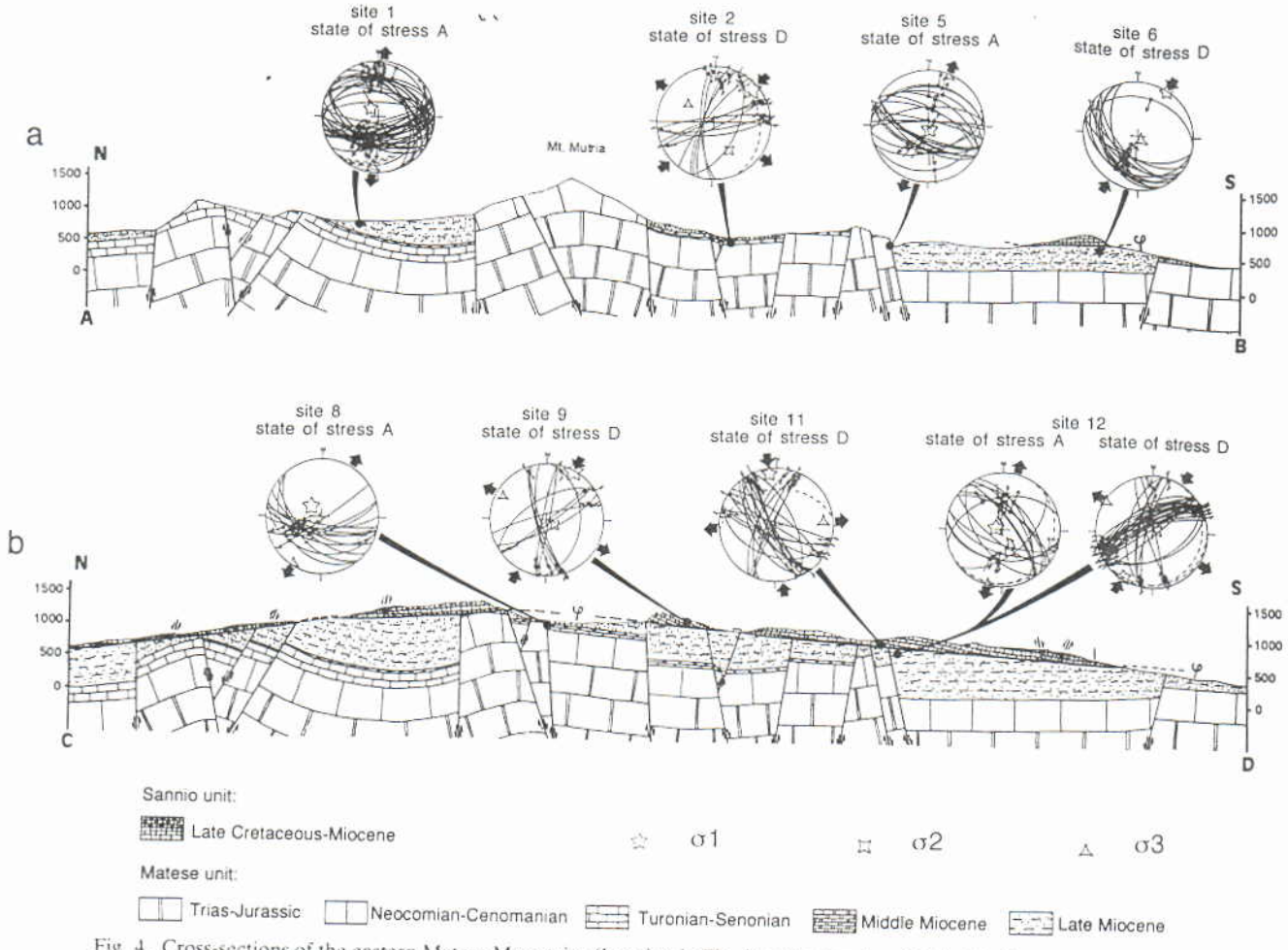

Fig. 4. Cross-sections of the eastern Matese Mountains (location in Fig. 3) and examples of Schmidt diagrams with faults and computed stress axes (see Table 1). Axes of computed palaeostress: five-branch star = σ_1, four-branch star = σ_2 and three-branch star = σ_3. In (a), normal faults with several hundred metre offsets are tilted within the folds. The major normal faults moved during NNE–SSW trending extension. In (b), the extensional structures of the Matese are sealed by the more recent Sannio back-thrust unit probably thrusted with NNE–SSW-trending compression.

these large normal faults, which have vertical separations of several hundred meters at the eastern limit of the Matese Mountains (Fig. 4a), is found in the Sannio unit. As shown in the cross-section of Fig. 4(b), the Sannio back-thrust (Fig. 3) seals the normal faulting structures of the Matese. This observation of major normal faults pre-dating major thrusts also confirms that in the Matese most of extensional deformation pre-dates compression.

For a better dating of these tectonic states of stress, we took into account the relations of the faults with the stratigraphy. Southeast of the Matese Mountains, the three compression trends (NNE–SSW, ESE–WNW and ENE–WSW) affect the Pliocene filling of piggyback basins (Fig. 1b). Northwest of the Matese Mountains (near Arpino, Fig. 1b), the ENE–WSW compression affects sediments as young as the early–middle Pleistocene. As for the Ofanto piggyback basin (Hippolyte *et al.* 1994b), these three compression trends are Pliocene–Quaternary in age, the oldest (NNE–SSW) being Pliocene or slightly older. Therefore, the normal faults predating the Pliocene–Pleistocene compression and affecting the Tortonian–Messinian flysch of the Matese Mountains, are late Miocene in age. Furthermore, the comparison between the large offsets on the E–W trending faults (several hundred metres) and the thickness variations of the late Miocene deposits (Fig. 4) suggests that this late Miocene normal faulting occurred during the deposition of the flysch sediments.

From the observation of normal faulting pre-dating compression and thrusting, we infer that the extension in the Matese Mountains cannot be considered as part of the Tyrrhenian extension that would have recently shifted into the mountain belt. This extension in the Matese is late Miocene in age, whereas the extension affecting the Tyrrhenian continental margin of the Southern Apennines is younger, mainly Pliocene–Pleistocene (Bartole *et al.* 1984).

As mentioned above, the major late Miocene extension of the Matese is very probably associated with deposition of the thick flysch formation of the same age. The western platform sedimentation comprised shallow-water carbonates since Jurassic times and changed to marls during the Serravallian, then to flysch during the late Miocene (Fig. 4). According to Casero *et al.* (1988), this change results from a rapid subsidence due to the shift of the foreland carbonate platform into a foredeep during the subduction process (Fig. 2). Effectively, the

Table 1. Palaeotress tensors computed from fault-slip data of the Matese mountains. Site localities are shown in Fig. 3. S = state of stress: A = NNE–SSW-trending extension; B = NE–SW-trending extension; C = NW–SE-trending extension; D = N–S to NNE–SSW-trending compression; E = ESE–WNW-trending compression; F = ENE–WSW-trending compression. N = number of faults used for tensor calculation. Stress axes: trend and plunge in degrees; $\phi = (\sigma_2 - \sigma_3)/(\sigma_1 - \sigma_3)$; Ang. = average angle between computed shear stress and observed slickenside lineation (in degrees)

Site	Age of rocks	S	N	Orientation of palaeostress σ_1	σ_2	σ_3	Φ	Ang.
1	Tortonian	E	20	287 05	042 78	196 11	0.62	09
		F	17	068 06	199 80	337 07	0.24	13
		D	16	033 08	283 69	126 20	0.22	08
		B	32	327 70	148 20	058 00	0.35	10
		C	35	341 77	232 04	141 12	0.44	09
2	Serravallian	A	41	318 74	093 11	186 11	0.52	07
3	Langhian	D	14	047 13	150 43	304 44	0.18	10
		D	16	193 14	311 62	096 24	0.42	07
4	Cretaceous	B	8	168 65	072 03	340 25	0.04	18
		F	10	070 07	161 03	271 82	0.35	08
5	Tortonian	C	4	333 75	211 08	119 13	0.35	05
6	Late Miocene	A	21	161 84	291 04	021 05	0.46	08
		D	23	032 03	302 03	169 86	0.46	07
		A	7	286 76	126 13	035 05	0.34	12
7	Tortonian	E	18	319 11	127 78	229 02	0.26	13
		C	10	023 77	208 13	298 01	0.42	13
		A	9	079 73	304 12	211 12	0.19	15
8	Cretaceous	D	19	046 27	182 55	305 21	0.22	11
		A	14	313 69	119 21	211 05	0.22	06
9	Cretaceous	C	12	207 81	053 08	322 04	0.38	07
		C	10	333 68	194 17	099 14	0.45	11
		D	13	028 02	127 76	298 14	0.14	14
10	Cretaceous	E	4	294 21	087 67	201 10	0.34	08
11	Cretaceous	C	13	006 80	236 06	145 07	0.70	06
		D	22	352 10	234 69	085 18	0.46	18
		C	19	168 77	032 09	300 09	0.37	09
12	Late Miocene	B	17	004 83	148 06	239 04	0.54	12
		A	16	286 80	104 10	194 00	0.37	10
		C	8	147 84	030 05	120 04	0.36	09
		D	35	212 04	076 84	302 04	0.33	10

SOLUTION 1:

A	Succession B	C	A	D	F	E
B		6		3	5	1
C				2	1	1
A				1	2	2
D					5	2
F						1
E						

SOLUTION 2:

	Succession B	A	C	D	F	E
B			6	3	5	1
A				1	2	2
C				2	1	1
D					5	2
F						1
E						

SOLUTION 3:

	Succession A	B	C	D	F	E
A				1	2	2
B			6	3	5	1
C				2	1	1
D					5	2
F						1
E						

Fig. 5. Chronologies for the three possible successions of states of stress identified in the eastern Matese Mountains (method: Angelier 1991). The table indicates the number of chronological relationships observed between the state of stress in a column and the state of stress in the line (A, B, C, D, E & F, as in Table 1). For the three possible successions, all extensional states of stress (A, B & C) pre-date all compressional states of stress.

Fig. 6. Example of normal faults pre-dating compression. (a) Conjugate normal faults offset by bedding-plane faults during folding (site 1 of Fig. 3). Some normal faults have a strike-slip motion overprinting the normal motion. With the bedding plane faults, they indicate NNE–SSW-trending compression. (b) Tilted conjugate normal faults in Miocene sandstones. During folding, the bedding plane and the normal faults (event 1) have been tilted (event 2; compare with a). The site is located in the Neogene folds of the eastern Sannio Mountains (Fig. 1b); similar structures were observed in the Matese Mountains. (c) Tilted normal fault (north of site 1, Fig. 3); S_0 = bedding plane; C = Cretaceous limestone; M = late Miocene marls. The bedding plane dips to the southeast (left-hand side). The late Miocene marls are downfaulted relative to Cretaceous limestone. Associated with the large fault are conjugated minor faults similar with those of (b) (not visible in this photograph) which indicate that this reverse fault is a tilted normal fault.

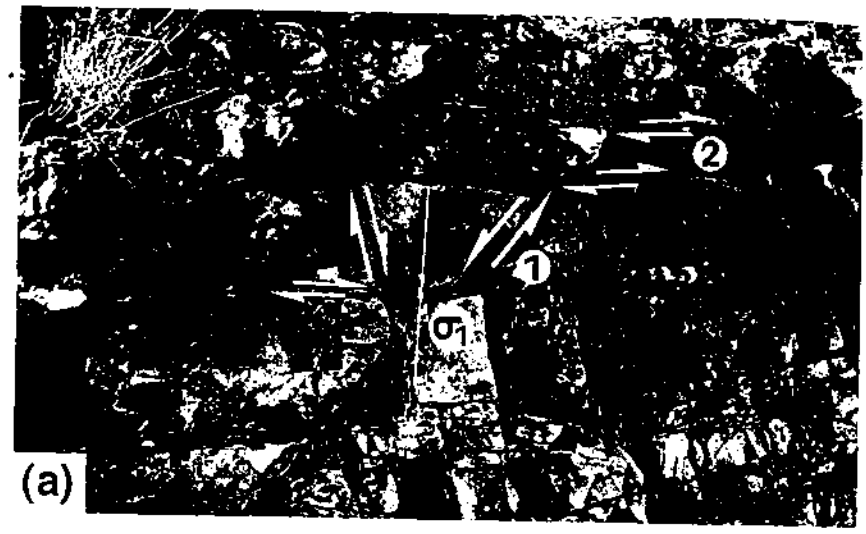
2
1
σ1
(a)

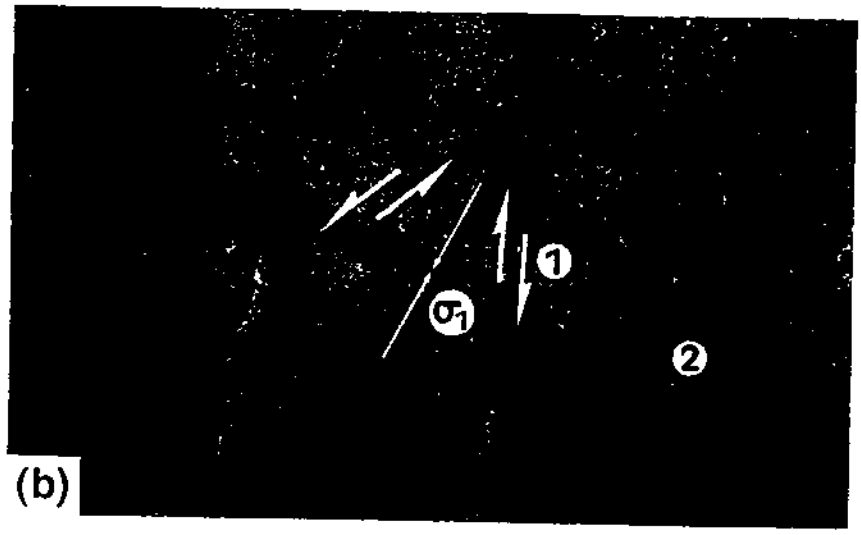
1
σ1
2
(b)


S
N
S0
C
(c)

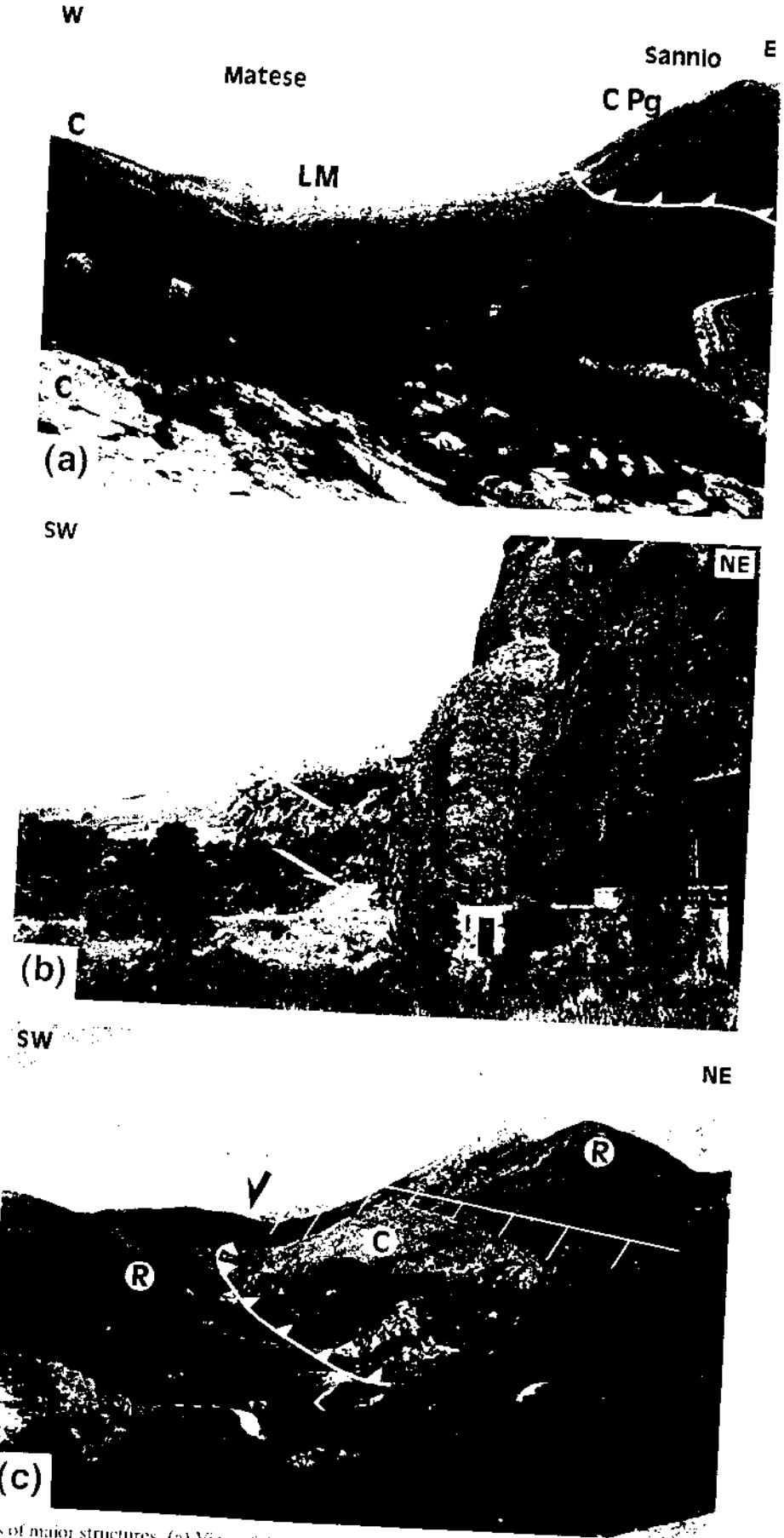

Fig. 7. Examples of major structures. (a) View of the Sannio unit overthrusting the Matese unit (close to site 9 of Fig. 3): C = Cretaceous limestone; LM = late Miocene marls (this stratigraphic unit contains olistoliths in its upper part); C, Pg = Cretaceous and Palaeogene limestone and conglomerate. The Matese Cretaceous limestone dips toward the Sannio unit. The white cliff in the Matese unit corresponds to the large normal fault south of the Mutria Mountain, scaled by the Sannio thrust unit (Figs. 3 and 4b). (b) Early Pleistocene sinistral strike-slip fault along the northern rim of the Sant'Arcangelo Basin (site 11 of Fig. 8). (c) Example of normal faulting post-dating thrust tectonics (Val D'Agri middle Pleistocene graben, located immediately West of Sant'Arcangelo Basin in Fig. 1). A klippe of Cretaceous carbonates (C, clear in the centre of photograph) belongs to the W.P.U. (Fig. 1) which is thrusted, even farther to the northeast, over radiolarites (R, dark on photograph) of the L.M.U. (Fig. 1). The thrust contact was cut by a normal fault which offsets the top of the radiolarite unit.

late Miocene flysch is very similar in facies with the foredeep bodies of Romagna sector (Richi Lucchi 1986). The thick turbidite deposits are overlain by a 'closure facies' made of olistostromes interbedded in the foredeep sediments. The olistoliths are made up not of local Mesozoic–Neogene faulted limestone, but red and black clays of allochthonous origin ('Argille Varicolori', Late Cretaceous–Paleogene; Dubois 1976). As in the Romagna sector, the olistostromes have probably detached from a large thrust front. In agreement with this interpretation, we observed that at the bottom of the 'closure facies' sequence, the allochthonous coloured clay material is intercalated in thin layers within the flysch, suggesting that the allochthonous units were still far away. In contrast, in the upper sequence, this material forms ovoid olistoliths, suggesting that the thrust unit has moved closer.

Following Casero *et al.* (1988), we believe that the late Miocene flysch formation is a foredeep sedimentary unit that originated in the flexure of a foreland carbonate platform, the western platform. In such a context, the late Miocene extension can be interpreted as resulting from this flexure connected with subduction processes (Figs 1b and 2: see the present structure of the foredeep basin). As palaeomagnetic studies of middle Miocene rocks have revealed a 20° counterclockwise rotation of the eastern Matese (Channell & Tarling 1975, Catalano *et al.* 1976, Iorio & Nardi 1988) and considering that this rotation probably occurred during accretion, one must back-rotate (i.e. clockwise) 20° the pre-accretional structures of the chain in order to reconstruct their initial trends. Therefore, the large Matese normal faults that developed during the foreland flexure process may have had an original trend closer to NW–SE than their present-day east–west orientation. This Miocene normal fault trend resembles that of the foreland normal faults (NW–SE to WNW–ESE) which strike parallel to the flexural axes of the present foredeep (Fig. 1b).

We conclude that compression affected the Matese platform unit after normal faulting, when this unit was tectonically accreted in the mountain belt at the end of the late Miocene or at the beginning of the Pliocene. We also found sites with extension pre-dating compression outside the Matese mountains: closer to the Tyrrhenian sea (between the Matese mountains and Naples; Hippolyte 1992) and in the eastern part of the Sannio mountains (Fig. 6b). All these observations suggest that any present unit of the mountain chain may have successively undergone extension and compression which occurred in quite different settings: firstly in the foreland and secondly in a thrust unit of the mountain belt.

EXTENSION CONTEMPORANEOUS WITH THRUSTING

As illustrated in the Matese case study, thrusting occurred in the western part of the present Apennines during the late Miocene–early Pliocene, while extension was active in the Vavilov Basin of the Tyrrhenian sea (Fig. 1a). Later, compression migrated eastward and finally created duplexes in the lower carbonate unit (eastern platform; Fig. 2) resulting in the formation of the Pliocene–Quaternary piggyback basins (Fig. 1b). Also during the Pliocene–Quaternary, the Salerne Basin (Moussat 1983) opened as a major graben of the Tyrrhenian Basin (Fig. 1). The Salerne Basin is of interest because it includes an inland part as the Sele Plain (Figs. 1b and 8). This part of the basin is filled up with about 1500 m of Pleistocene clastic continental sediments (Ippolito *et al.* 1973, Ortolani & Torre 1981). We could study outcrops of faulted Pleistocene conglomerates, especially in the Eboli sedimentary unit where K/Ar dating of 1.5 ± 1.25 Ma (Cinque *et al.* 1988) and pollens from Tiglian times (Gars 1983) indicate an early Pleistocene age.

In this area, the Quaternary normal faults clearly post-date Miocene thrusting and folding (Bartole *et al.* 1984, Fusi & Garduno 1992). The WSW–ENE trending normal faults of the Sele Plain constitute the inland prolongation of the northern border faults of the Salerne graben (Fig. 8) and are therefore related to the Tyrrhenian opening. Note that in this area and in the Mesozoic units of the Sorrentino Peninsula, numerous normal faults have similar WSW–ENE trends (Gars 1983, Cello *et al.* 1982, Fusi & Garduno 1992).

Many sites in the Mesozoic and Tertiary sediments around the Sele Plain show strike-slip and reverse faults, indicating NNE–SSW to NNW–SSE trending compression (Capotorti & Tozzi 1991, Hippolyte 1992). In contrast, no reverse fault was found in the Quaternary sediments, where we could observe normal faults. These Quaternary normal faults result from a NNW–SSE trending extension (e.g. site 3, Fig. 8 and Table 2). At the foot wall of some faults, olistoliths of consolidated conglomerates indicate that normal faulting was syndepositional. It confirms that this Pleistocene extensional tectonism is contemporaneous with the opening of the Salerne graben.

Some minor fault planes also indicate the existence of strike-slip regime (Gars 1983) with σ_1 axes trending ENE–WSW and σ_3 axes trending NNW–SSE (e.g. sites 2, 4, 5 & 6; Fig. 8 and Table 2). Since the extension direction, NNW–SSE, is common to extensional and strike-slip regimes, we infer that these two states of stress are related through a permutation of stress axes σ_1 and σ_2 (Angelier & Bergerat 1983). Such permutations may occur quickly (Hippolyte *et al.* 1992), and these two regimes are probably more or less simultaneous. This means that, during the dominant NNW–SSE extension, some ENE–WSW confining pressure existed.

During the opening of the Salerne graben on the Tyrrhenian margin of the Apennines, and thus during early Pleistocene, the Sant'Arcangelo, Metaponto and Amendolora piggyback basins formed on the front of the fold-and-thrust belt (Fig. 8). Effectively, reverse and strike-slip faults affect early Pleistocene deposits in this frontal area (Catalano *et al.* 1993). Moreover, we showed (Hippolyte 1992, Hippolyte *et al.* 1994b), in the case of faults controlling basin formation, that these

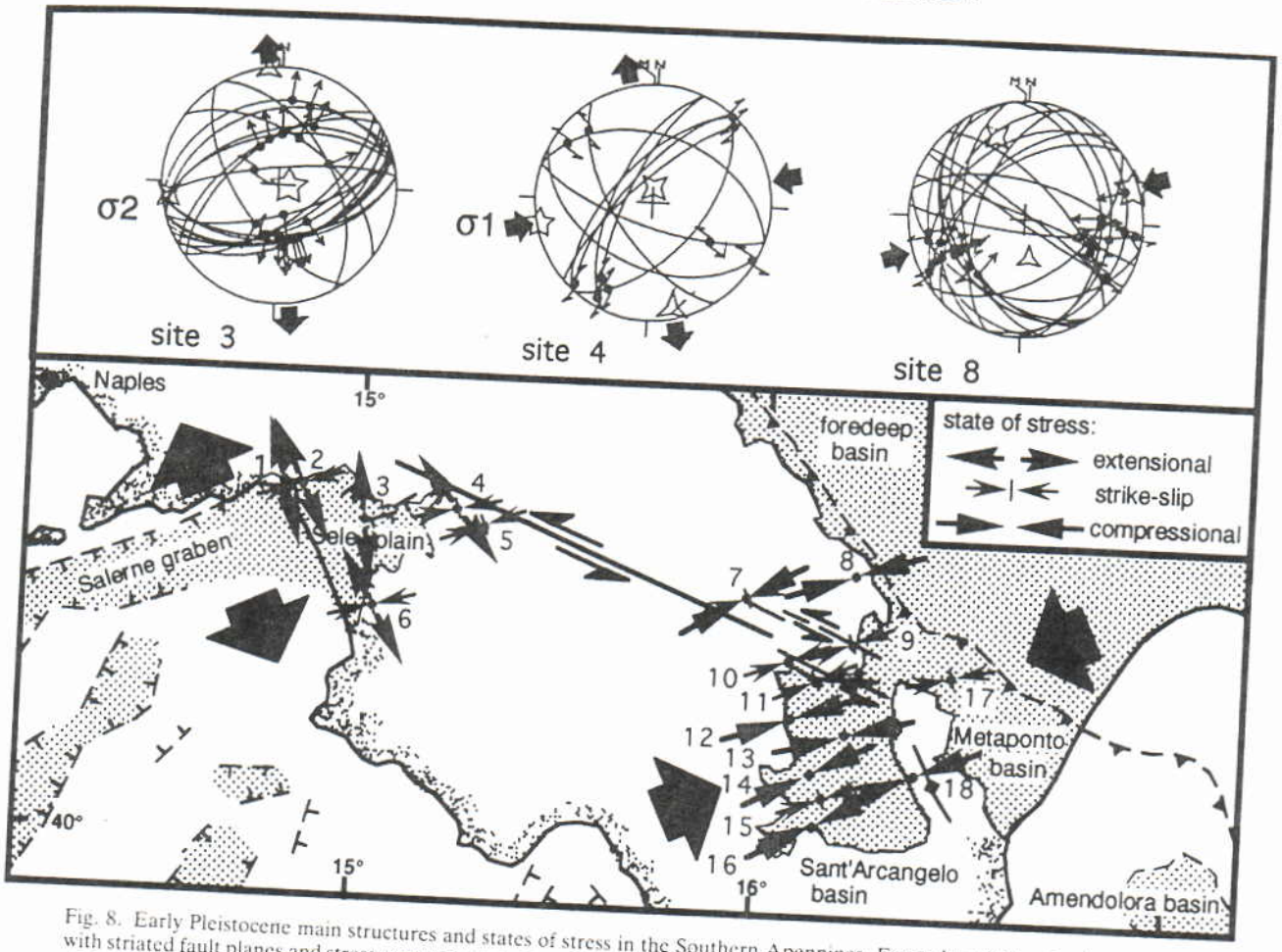

Fig. 8. Early Pleistocene main structures and states of stress in the Southern Apennines. Examples of Schmidt diagrams with striated fault planes and stress axes representative of the eastern, central and western areas. Compare the stress fields of the Tyrrhenian side of the belt (Salerne graben) and the one of the front of the belt (Sant'Arcangelo and Metaponto piggyback basins). These two areas are probably connected by a strike-slip fault system prolonging the sinistral strike-slip faults identified north of the Sant'Arcangelo Basin.

Table 2. Palaeostress tensors for site localities of Fig. 8. Same legend as in Table 1; T = type of event: E = normal faulting; S = strike-slip faulting; C = reverse faulting

Site	Age of rocks	T	N	Orientation of palaeostress σ_1	σ_2	σ_3	Φ	Ang.
1	Messinian	E	19	049 76	257 12	165 06	0.58	06
2	Early Pleist.	E	18	248 76	064 14	154 01	0.51	10
		S	16	073 15	221 72	341 09	0.40	11
3	Early Pleist.	E	20	097 83	263 07	353 02	0.30	09
4	Pliocene	S	10	257 03	003 80	167 10	0.58	08
		E	10	265 87	051 02	141 01	0.44	12
5	Pliocene	S	18	249 02	359 83	159 06	0.22	12
6	Aquitanian	S	37	253 01	162 72	343 18	0.33	12
		E	06	185 75	061 09	329 13	0.56	06
7	Late Pliocene	S	13	250 18	036 69	156 11	0.15	12
		C	07	060 04	329 11	168 79	0.61	10
		E	04	256 76	067 13	157 02	0.48	15
8	Pliocene	C	22	072 05	339 27	172 63	0.23	10
9	Early Miocene	S	22	248 02	150 77	338 13	0.21	10
10	Eocene	S	11	069 11	214 77	337 07	0.35	10
11	Pliocene	S	14	245 01	338 76	155 14	0.16	16
12	Early Pleist.	C	06	251 27	348 12	099 60	0.53	07
13	Early Pleist.	C	26	255 03	163 33	350 57	0.20	13
14	Early Pleist.	C	17	063 03	157 53	331 37	0.12	08
15	Early Pleist.	S	14	250 09	098 80	341 05	0.62	16
16	Pliocene	C	34	062 03	153 12	318 77	0.04	09
17	Early Pliocene	S	05	257 23	013 47	150 35	0.20	20
18	Early Pliocene	C	09	068 14	169 38	322 48	0.26	15

faults do not post-date early Pleistocene but were active during deposition of the thick early Pleistocene sediments. Palaeostress analysis in these early Pleistocene basins reveals that, depending on the location, strike-slip or reverse regimes prevailed during early Pleistocene with σ_1 axes trending ENE–WSW for both regimes (Fig. 8).

Comparing this early Pleistocene compression direction (σ_1) at the front of the belt with the early Pleistocene orientation of the maximum horizontal stress axes (σ_2 or σ_1) in the Sele Plain, one observes that they are the same (ENE–WSW). This particular stress field, with the same orientation of the maximum and minimum horizontal stress axes for different state of stress (Fig. 8) suggests that a gradient of stresses existed from the back-arc basin to the front of the mountain chain. The ENE–WSW trending stress axis was σ_2 to the west and σ_1 to the east.

Note that the Tyrrhenian extension was identified close to the Tyhrrhenian coast. In the mountain chain, not all faults of NNW–SSE extension can be related to the Tyrrhenian opening. In this area, some slip indicators on low angle normal faults are considered to be a response to thrust belt arcuation (Oldow *et al.* 1993) or to lateral stretching in the subducted slab (Doglioni 1991). In contrast, the high angle normal faults we measured in the Salerne graben are clearly related to the Tyrrhenian opening. This graben belongs to the Tyrrhenian graben system and the normal faults can be dated with good confidence of the Marsili Basin opening period, since they are found in the early Pleistocene sediments where they are syn-depositional. The direction of extension in the Salerne graben (NNW–SSE) is comparable with the probable opening direction of the Marsili Basin (N110/130E, see Sartori 1989; fig. 1a) and arise from the Tyrrhenian geodynamics.

In the Southern Apennines, the early Pleistocene thrust movement at the front of the belt is larger in the southeast than in the northwest. The thrust front did not move in the Molise area (Fig. 1b) (Casnedi *et al.* 1982). Its motion, still minor (300 m) at about latitude 41°20′ (Casnedi *et al.* 1982, Casero *et al.* 1991) increases to the southeast with 2 km at latitude 40°40′ (Casnedi *et al.* 1982, Casero *et al.* 1991) and about 4.5 km east of Sant'Arcangelo Basin at latitude 40°20′ (Balduzzi *et al.* 1982). It is noteworthy that all Pleistocene piggyback basins of the Southern Apennines are located in this area of maximum Pleistocene thrusting (Sant'Arcangelo, Metaponto and Amendolora basins; Figs 1b and 8). North of these basins, we have identified major left lateral strike-slip faults (Figs 8 and 7b). One of these faults offsets Pliocene folds of 2.5 km (close to site 9 of Fig. 8) (Hippolyte 1992, Catalano *et al.* 1993). Those faults moved during the same ENE–WSW compression that formed the Pleistocene piggyback basins (Fig. 8). They have probably induced the larger Pleistocene displacement of the southern thrust units.

Similarly, during the early Pleistocene, extension in the Tyrrhenian Basin mainly occurred in its southernmost part (Marsili Basin; Fig. 1a) (Kasten *et al.* 1990). The Salerne graben is among the northernmost Pleistocene extensional structures (Fig. 1b). It is possible that strike-slip faults prolonging those identified north of the Sant'Arcangelo Basin connect the northern border of these two areas of unusual Pleistocene tectonic activity (Fig. 8). Similarly, note in Fig. 1 that the Salerne graben ends to the west against another sinistral strike-slip fault identified offshore (Moussat 1983). The onshore WNW–ESE trending transfer fault system shown in Fig. 8 constitutes the boundary of a southern block that moved to the southeast relative to the rest of the Apennines, along the strike of the faults and parallel to the opening direction of the Marsili Basin proposed by Sartori (1989). This block displacement can account for the kinematic relationships between extension in the Tyrrhenian area and compression on the front of the mountain chain.

In conclusion, extension in the western part of the mountain chain, contemporaneous with thrusting in the eastern part, is well characterized for the early Pleistocene time because it was possible to carry out tectonic analyses in an onshore part of a Tyrrhenian graben. The mechanism allowing the transition from extensional to compressional movement is probably a strike-slip transfer faulting, difficult to identify in the highly deformed, clayey units of the mountain chain but easier to recognize north of the Sant'Arcangelo Basin (Figs. 7b and 8). This tectonic pattern of the Southern Apennines can be compared with models made for Calabria that consider major WNW–trending left lateral strike-slip faults (e.g. Moussat 1983, Knott & Turco 1991). In the Southern Apennines, we show that the stress field is characterized by an ENE–WSW maximum horizontal stress axis with an east–west stress gradient from the back-arc region to the front of the belt.

EXTENSION POST-DATING THRUSTING

As shown before, whereas extension of the Tyrrhenian margin is superimposed on compressional structures, it did not post-date all of the compression of the belt, but occurred contemporaneously with thrust activity on the eastern border of the mountain chain. We also demonstrate that some extensional structures truly post-date compression in the Southern Apennines.

In the study area (Fig. 1b), no compression was found to be younger than early Pleistocene. The tectonic contact between the Apenninic thrust sheets and the early Pleistocene foredeep sediments is sealed by post-orogenic Sicilian clastic deposits (Ogniben 1969) (Figs. 1b and 2). The upper sediments of the early Pleistocene piggyback basins remain unfolded. Finally, no focal mechanism supports the existence of compression in this area (Fig. 9).

On the other hand, stress determination using measurements of faults formed during the 1982 Irpinia earthquake and other faults, either with Holocene scarps or cutting middle Pleistocene–Holocene sediments, indicate only extension, which is presently trend-

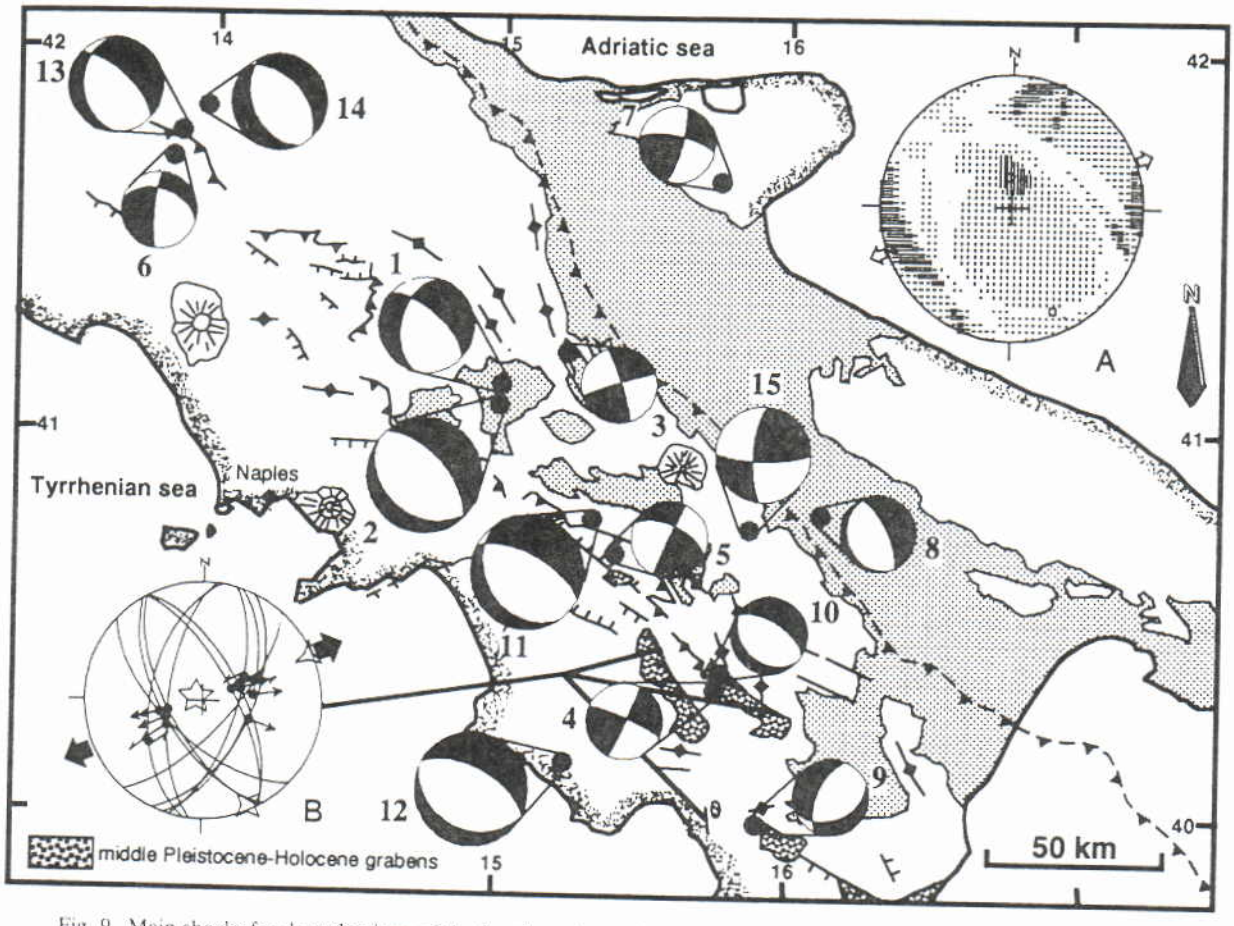

Fig. 9. Main shocks focal mechanisms of the Southern Apennines (see Table 3). Schmidt diagram (a): present synthetic stress tensor deduced using the right dihedron method and representative of the Southern Apenninic mountain (focal plane mechanisms 13, 6, 14, 1, 2, 11, 5, 12, 4, 10 & 9). Schmidt diagram (b): example of middle Pleistocene–Holocene stress tensor determined from inversion of fault-slip data measured on the field (middle Pleistocene–Holocene grabens; Hippolyte *et al.* 1994a).

ing NE–SW (ranging between N10E and N70E, Hippolyte *et al.* 1994a). These directions seem to be compatible with the orientations of the *T*-axes of earthquake focal mechanisms (Cello *et al.* 1982) (Fig. 9). However, the orientation of the *T*- and P-axes correspond to the σ_3 and σ_1 stress axes only in particular cases (McKenzie 1969). We have used the right dihedron method (Angelier & Mechler 1977) to determine a present stress tensor from the existing focal plane mechanisms and to allow its comparison with the middle Pleistocene–Holocene stress field determined by inversion of fault-slip orientations by Hippolyte *et al.* (1994a). This right dihedron method is based on the statement that, for each focal plane mechanism, σ_1 belongs to a compressional right dihedron and σ_3 belongs to an extensional one. Provided that the axes σ_1 and σ_3 have the same orientation for all focal mechanisms, the diagram area common to all compressional dihedrons contains σ_1 while that common to all extensional dihedrons contains σ_3. The compatibility areas and their barycentres are thus defined, as in diagram A of Fig. 9.

The idea to use focal mechanisms for such a large area is supported by the homogeneity of the stress field determined with fault-slip field measurements (Hippolyte *et al.* 1994a). Among the available focal plane mechanisms of main shocks (Fig. 9, Table 3), some have hypocentres deeper than 15 km and belong to the underlying plate (locations 7, 3, 15 & 8). The remaining hypocentres belong to the upper plate and especially to the overthrust belt which was deformed by compression during Pliocene–Quaternary time (Fig. 2). To obtain a stress tensor representative of the deformation within the belt, we used this second set of focal mechanisms exclusively. The resulting high probability areas (90–100%) for σ_1 and σ_3 are shown as dark areas in Fig. 9a. The vertical attitude of the inferred σ_1 stress axis confirms that the stress regime of this Pliocene–Quaternary compressional area is extensional. The probable σ_3 stress axis is trending N69E. This result is consistent with the Quaternary stress field obtained with fault planes (Fig. 9b). It is also consistent with the stress orientation determined with aftershock focal mechanisms of the 1982–1985 crisis in the Phlegrean Napolitan volcanic caldera (N12E, Zuppetta & Sava 1991), and with the aftershock of the Irpinia earthquake (ENE–WSW, Julien & Cornet 1987; N49E, Mercier & Carey-Gailhardis 1989).

Accordingly, the present extension (NE–SW) strongly differs from the Pleistocene one (NNW–SSE). Not only the direction, but also the area affected, are different. Whereas the NNW–SSE extension was mostly developed on the Tyrrhenian margin (Fig. 8), the pres-

Table 3. References of focal plane mechanisms in Fig. 9. N = reference number; P_t = trend of P-axis; P_p = plunge of P-axis; T_t = trend of T-axis; T_p = plunge of T-axis. References: We = Westaway 1987; Ga = Gasparini *et al.* 1985; Ce = Cello *et al.* 1982; We–Ja = Westaway & Jackson 1987; Dz = Dziewonski *et al.* 1985, 1988, 1991

N	Date	Time	Latitude	Longitude	Depth	Magnitude	P_t–P_p	T_t–T_p	Reference
01	21-08-1962	18:09	41.119	15.018	08	5.7	172–52	068–11	We 1987
02	21-08-1962	18:19	41.084	15.002	08	6.1	186–64	055–18	We 1987
03	06-05-1971	03:45	41.200	15.240	33	4.8	297–02	207–07	Ce 1982
04	29-11-1971	18:49	40.340	15.770	04	4.7	158–03	248–08	Ga 1985
05	08-08-1973	14:36	40.720	15.410	05	4.6	256–28	154–22	Ga 1985
06	30-10-1973	01:14	41.700	13.870	05	4.4	134–39	244–22	Ga 1985
07	19-06-1975	10:11	41.650	15.730	18	4.9	147–05	239–21	Ga 1985
08	24-09-1978	08:07	40.797	16.109	28	4.2	238–63	066–26	Ga 1985
09	09-03-1980	12:00	39.990	15.910	10	4.3	066–64	312–11	Ce 1982
10	14-05-1980	01:40	40.360	15.770	15	4.2	197–74	034–16	Ce 1982
11	23-11-1980	18:34	40.778	15.332	10	6.9	241–75	043–14	We–Ja 1987
12	16-01-1981	00:37	40.130	15.230	15	8.5	212–75	027–15	Dz 1988
13	07-05-1984	17:49	41.765	13.898	10	5.8	189–63	057–19	Dz 1985
14	11-05-1984	10:41	41.831	13.961	14	5.2	164–80	056–03	Dz 1985
15	05-05-1990	07:21	40.750	15.850	26	5.7	138–03	046–21	Dz 1991

ent NE–SW extension is mostly active within the axial belt (Fig. 9). There, several grabens elongated NW–SE and filled up with lacustrine sediments (Fig. 9) were created, starting up in the early–middle Pleistocene (around 0.8 Ma, Cinque *et al.* 1993). Most of these extensional structures are probably still active since they are generated by the same stress field as the present one (NE–SW extension; diagram B of Fig. 9). Moreover, the age of their initiation coincides with the age of the last thrusting on the front of the belt and therefore allows dating the stress field change of early–middle Pleistocene. This conclusion, based on palaeostress reconstruction and focal plane mechanisms analysis, is an alternative of previous interpretations, where either a dominant strike-slip tectonics is considered for this middle–late Pleistocene period (Catalano *et al.* 1993) or a NE–SW extension is noted but considered contemporaneous with thrusting (e.g. Doglioni 1991, Oldow *et al.* 1993) and is related to back-arc extension despite the large difference in trend with the Tyrrhenian extension (Sartori 1989).

The recent change in the stress field underlines the contrast between Present and Miocene–Quaternary tectonics. A process markedly different from the subduction must have induced this new regime. In that sense, it is noteworthy that the present geodynamic is characterized by a strong post-Calabrian uplift (reaching 700 m) of the mountain chain and of the foredeep which was previously subsiding. The extension that post-dates thrusting and is now active in the Southern Apennines (Fig. 9) is thus interpreted as resulting from the late uplift and bending of the thrust stack. Note that the distribution of Quaternary sediments within the northern and central Apennine foredeep basin independently suggested to Kruse & Royden (1994) that a fundamental change in the subduction process occurred in early Quaternary time. Modelling by these authors indicates that an unbending of the North Adriatic lithosphere, following its progressive bending during Pliocene time, may be the result of a reduction in the loads acting on the subducted lithosphere at mantle depths. The reason for this release of strain energy may be a complete detachment of a subducting lithosphere slab (Göler & Giese 1978, Spakman 1990, Van Dijk & Okkes 1990, Cinque *et al.* 1993).

CONCLUSION

The various phases of deformation documented in the Southern Apennines can be related to the evolution of a thrust unit in an accretionary model, and to the change in the geodynamic evolution of the mountain chain (from extension/compression related to a subduction process, to mere extension of the uplifted chain).

The observed mixture of compressional and extensional structures may provide the wrong image of frequent alternating compressive and distensive phases. In fact, this complexity results from the continuous evolution of thrust units which are deformed at their successive position in the arc system, which itself is characterized by a geographic zonation with extension in a foredeep basin, compression in the mountain chain and extension in the back-arc basin (Fig. 10).

Similarly, the superposition of extensional structures with different trends may provide the wrong image of radial extension, considered as typical of most back-arc areas (Angelier & Bergerat 1983, Bousquet & Philip 1986). Concerning the Pleistocene deformation in the Southern Apennines, we demonstrate that the juxtaposition of sub-perpendicular grabens (Fig. 1b) is fortuitous and corresponds to NW–SE structures of the present extension resulting from bending of the crust, and previous ENE–WSW structures of the Tyrrhenian Basin opening.

Our analyses bring some information on the space and time distribution of stresses to help in an understanding of the origin of back-arc basins (e.g. Uyeda 1986, Malinverno & Ryan 1986). We show that for the early Pleistocene, the relation between the Apenninic and the Tyrrhenian back-arc stress fields is relatively simple since, in both areas, the maximum and minimum horizontal stresses have similar directions (ENE–WSW and

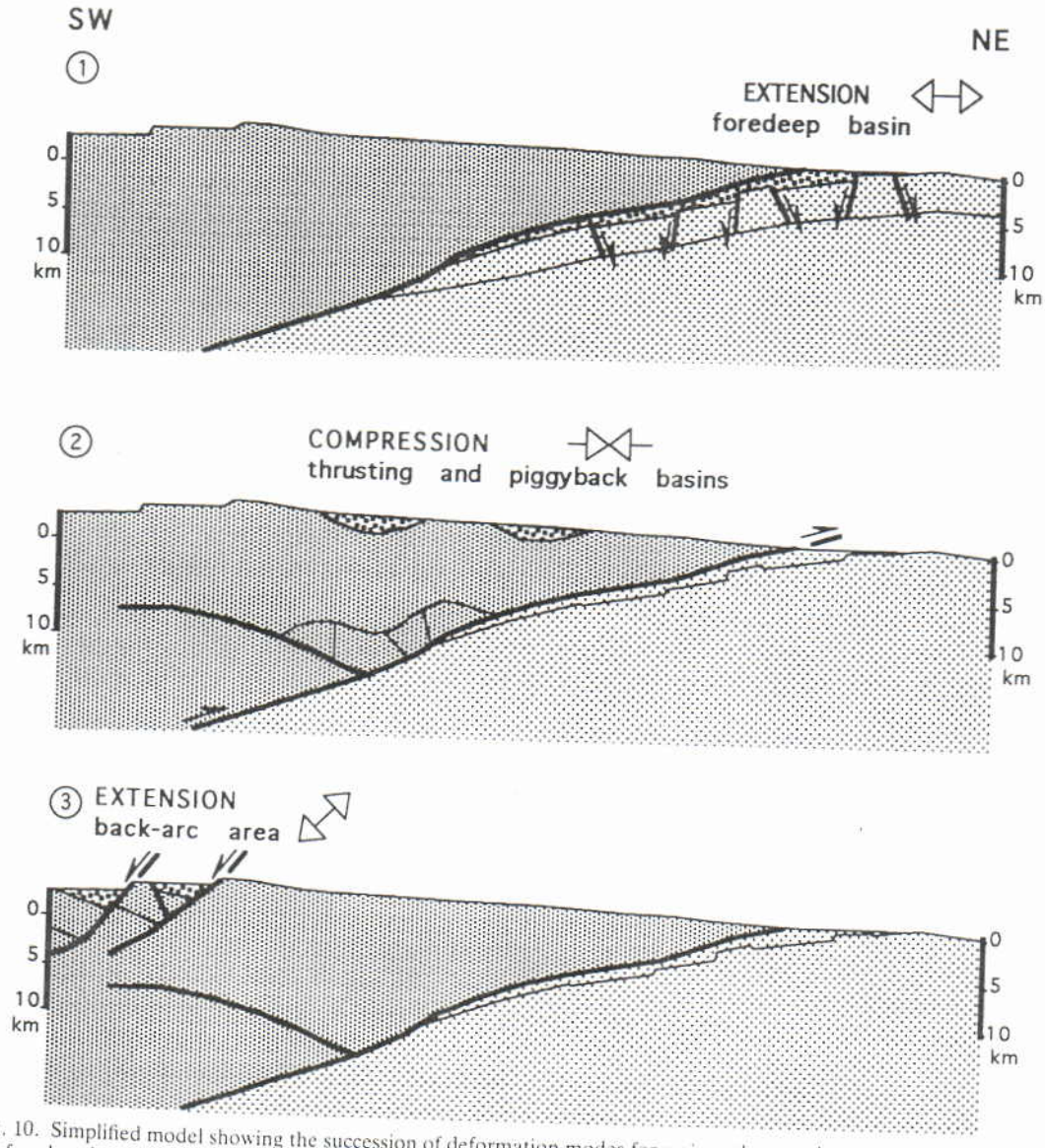

Fig. 10. Simplified model showing the succession of deformation modes for a given thrust unit: 1, ~NE–SW extension in the foredeep basin; 2, ~NE–SW compression in the thrust belt; 3, ~NW–SE extension in the back arc area. Note that the NE–SW-trending stress axis is σ_3 in the foredeep, σ_1 in the mountain chain and σ_1 (strike-slip regime) or σ_2 (extensional regime) in the back-arc basin.

SSE–NNW, respectively; Fig. 8). The difference between those two areas is that the maximum horizontal stress is σ_1 near the front of the belt and σ_2 in the back-arc basin. The orientation of σ_3 in the back-arc basin (NNW–SSE) is perpendicular to the direction of σ_1 determined at the front of the mountain chain and subparallel to the opening direction of the Marsili Basin (Fig. 1a).

In the Southern Apennines, such characteristics of the stress field may also have existed for previous periods (late Miocene–Pliocene), when extension was active in the Vavilov Basin (Fig. 1a) in an east–west direction (Kasten *et al.* 1990) and compression was nearly perpendicular in Northern Apennines (NNE–SSW: Fesce 1986), in the Southern Apennines (NNW–SSE to NNE–SSW: Hippolyte 1992) and in Sicily (north–south to NNE–SSW: Ghisetti 1979, Barrier 1992).

We conclude that, despite apparent complexity, the succession of compressional and extensional states of stress is relatively simple in the Southern Apennines. The interpretation of these typical examples does not require, for instance, alternating locking and unlocking of the subduction fault, but can be integrated in a single evolving subduction model, provided that the Quaternary major change is taken into account.

REFERENCES

Angelier, J. 1989. From orientation to magnitudes in paleostress determinations using fault slip data. *J. Struct. Geol.* **11**, 37–50.

Angelier, J. 1991. Analyse chronologique matricielle et succession régionale des événements tectoniques. *C. r. Acad. Sci. Paris* **312**, 1633–1638.

Angelier, J. & Bergerat, F. 1983. Systèmes de contrainte et extension intracontinentale. *Bull. Centres Rech. Explor.-Prod. Elf-Aquitaine* **7**, 137–147.

Angelier, J. & Mechler, P. 1977. Sur une méthode graphique de recherche des contraintes principales également utilisables en tectonique et séismologie: la méthode des dièdres droits. *Bull. Soc. géol. Fr.* **7** *ser.* 1309–1318.

Auroux, C. 1984. Evolution néotectonique de la Dorsale Apulienne et de ses bordures. Unpublished thesis, Université de Nice, Tome I, 138 pp.

Balduzzi, A., Casnedi, R., Crescenti, U., Mostardini, F. & Tonna, M.

1982. II Plio-Pleistocene del sottosuolo del Bacino Lucano (Avanfossa Appenninica). *Geol. Romana* **21**, 89–111.
Barrier, E. 1992. Tectonic analysis of a flexed foreland: the Ragusa Platform. *Tectonophysics* **206**.
Bartole, R., Savelli, D., Tramontana, M. & Wezel, F. 1984. Structural and sedimentary features in the Tyrrhenian margin of Campania, Southern Italy. *Mar. Geol.* **55**, 163–180.
Bernini, M., Boccaletti, M., Moratti, G., Papani, G., Sani, F. & Torelli, L. 1990. Episodi compressivi Neogenico–Quaternari nell'area estensionale tirrenica nord-orientale. Dati in mare e a terra. *Mem. Soc. geol. It.* **45**, 577–589.
Boccaletti, M., Calamita, F., Centamore, E., Deiana, G. & Dramis, F. 1983. The Umbria–Marche Apennine: an example of thrusts and wrenching tectonics in a model of ensialic Neogenic–Quaternary deformation. *Boll. Soc. geol. ital.* **102**, 1–12.
Boccaletti, M., Nicolich, R. & Tortorici, L. 1984. The Calabrian arc and the Ionian Sea in the dynamic evolution of the Central Mediterranean. *Mar. Geol.* **55**, 219–245.
Bortolotti, V., Passerini, P., Sagri, M. & Sestini, G. 1970. The miogeosynclinal sequences. *Sediment. Geol.* **4**, 341–344.
Bousquet, J. C. & Philip, H. 1986. Neotectonics of the Calabrian Arc and Apennines (Italy): an example of Plio–Quaternary evolution from island arcs to collisional stage. In: *The Origin of Arc* (edited by Wesel, C. F.). Elsevier, Amsterdam, 305–326.
Capotorti, F. & Tozzi, M., 1991. Tettonica trascorrente nella penisola Sorrentina. *Mem. Soc. geol. ital.* **47**, 235–249.
Casero, P., Roure, F., Moretti, I., Muller, C., Sage, L. & Vially R. 1988. Evoluzione geodinamica neogenica dell'Appennino Meridionale. In: *L'Appennino Campano–Lucano nel Quadro Geologico dell'Italia Meridionale*. Atti del 74° Congresso. *Soc. geol. ital.* Sorrento, 13–17 settembre 1988 (edited by De Frede). Napoli, Relazioni, pp. 59–66.
Casero, P., Roure, F. & Vially, R. 1991. Tectonic framework and petroleum potential of the Southern Apennines. In: *Generation, Accumulation and Production of Europe's Hydrocarbons* (edited by Spencer, A. M.). Oxford University Press, 381–387.
Casnedi, R., Crescenti, U. & Tonna, M. 1982. Evoluzione della Avanfossa Adriatica Meridionale nel Plio–Pleistocene sulla base di dati di sottosuolo. *Mem. Soc. geol. ital.* **24**, 243–260.
Catalano, R., Channell, E. T., D'Argenio, B. & Napoleone, G. 1976. Mesozoic paleogeography of the Southern Apennines and Sicily. *Mem. Soc. geol. ital.* **15**, 95–118.
Catalano, S., Monaco, C. & Tortorici, L. 1993. Pleistocene strike-slip tectonics in the Lucanian Apennine (southern Italy). *Tectonics* **12**, 656–665.
Ceilo, G., Guerra, I., Tortorici, L., Turco, E. & Scarpa, R. 1982. Geometry of the neotectonic stress field in southern Italy: geological and seismological evidence. *J. Struct. Geol.* **4**, 385–393.
Channell, J. E. T. & Tarling, D. H. 1975. Palaeomagnetism and rotation of Italy. *Earth Planet. Sci. Lett.* **25**, 177–188.
Cinque, A., Guida, F., Russo, F. & Santangelo, N. 1988. Dati cronologici e stratigrafici su alcuni depositi continentali della Piana del Sele (Campania): i 'Conglomerati di Eboli'. *Geogr. Fis. Dinam. Quat.* **11**.
Cinque, A., Patacca, E., Scandone, P. & Tozzi M. 1993. Quaternary kinematic evolution of the Southern Apennines. Relationships between surface geological features and deep lithospheric structures. *Annal. Geofis.* **36**, 249–260.
Clermonté, J. & Pironon, B. 1979. La plate-forme Campano–Abruzzaise de la Méta au Matèse (Italie Méridionale): Différentiations au Paléogène et au Miocène, structures, relations avec les formations Molisanes. *Bull. Soc. géol. Fr.* 7 *ser.* **21**, 737–743.
Doglioni, C. 1991. A proposal for the kinematic modelling of W-dipping subductions—possible applications to the Tyrrhenian–Apennines system. *Terra Nova* **3**, 423–434.
Dubois, R. 1976. La suture Calabro–Apenninique crétacée-éocène et l'ouverture Tyrrhénienne néogène, étude pétrologique et structurale de la Calabre Centrale. Unpublished thesis, Université Paris 6.
Dziewonski, A. M., Ekstrom, G., Franzen, J. E. & Woodhouse, J. H. 1988. Global seismicity of 1981: centroid-moment tensor solutions for 542 earthquakes. *Phys. Earth & Planet. Interiors* **50**, 155–182.
Dziewonski, A. M., Ekstrom, G., Woodhouse, J. H. & Zwart, G. 1991. Centroid-moment tensor solutions for April–June 1990. *Phys. Earth & Planet. Interiors* **66**, 133–143.
Dziewonski, A. M., Franzen, J. E. & Woodhouse, J. H., 1985. Centroid-moment tensor solutions for April–June 1984. *Phys. Earth & Planet. Interiors* **37**, 87–96.
Fesce, A. M. 1986. Analisi micro e mesostrutturale dei conglomerati Neogenici e Pleistocenici del margine Appenninico fra il Bolognese e la Val Marecchia. Ricostruzioni tensoriali. Dottorato di Ricerca, Università di Bologna e di Modena, 212 pp.
Finetti, I. & Del Ben, A. 1986. Geophysical study of the Tyrrhenian opening. *Boll. Geof. Teor. Appl.* XXVIII **110**, 9–47.
Fusi, N. & Garduno, H. 1992. Structural analysis of a sector of the Tyrrhenian margin of the Southern Apennines: the horst of Sorrentina peninsula and Lattari mounts (Campania, Italy). *C. r. Acad. Sci. Paris* **315**, Sér. II, 1747–1754.
Gars, G. 1983. Etude sismotectonique en Méditerranée Centrale et Orientale: I. La tectonique de l'Apennin Méridional et le séisme (2 nov. 1980) de l'Irpinia (Italie). II. Les failles activées par les séismes (fev.–mars 1981) de Corinthie (Grèce). Unpublished thesis, Université de Paris-Sud Orsay.
Gasparini, C., Iannaccone, G., & Scarpa, R. 1985. Fault-plane solutions and seismicity of the Italian Peninsula. *Tectonophysics* **117**, 59–78.
Ghisetti, F. 1979. Relazioni tra strutture e fasi trascorrente e distensive lungo i sistemi Messino–Fiumefreddo, Tindari–Letojanni e Alia–Malvagna. (Sicilia nord-orientale): uno studio microtettonica. *Geol. Romana* **18**, 23–58.
Ghisetti, F. & Vezzani, L. 1981. Contribution of structural analysis to understanding the geodynamic evolution of the Calabrian arc (southern Italy). *J. Struct. Geol.* **3**, 371–381.
Göler, K. & Giese, P. 1978. Aspects of the evolution of the Calabrian Arc. In: *Alps, Apennines, Hellenides* (edited by Closs H., Roeder D. & Schmidt K.). *Sci. Rep.* **38**, 374–388, IUCG, Stuttgart.
Haccard, D., Lorenz, C. & Grandjacquet, C. 1972. Essai sur l'évolution tectogénétique de la liaison Alpes–Apennines (de la Ligurie à la Calabre). *Mem. Soc. geol. ital.* **11**, 309–341.
Hippolyte, J.-C. 1992. Tectonique de l'Apennin méridional: structures et paléocontraintes d'un prisme d'accrétion continental. Unpublished Ph.D. thesis, *Mém. Sci. Terre* **92–5**, Université P. et M. Curie, Paris.
Hippolyte, J.-C., Angelier, J. & Roure, F. 1992. Les permutations de contraintes dans un orogène: exemple des terrains quaternaires du sud de l'Apennin. *C. r. Acad. Sci. Paris* **315**, 89–95.
Hippolyte, J.-C., Angelier, J. & Roure, F. 1994a. A major geodynamic change revealed by Quaternary stress patterns in the Southern Apennines (Italy). *Tectonophysics* **230**, 199–210.
Hippolyte, J.-C., Angelier, J., Roure, F. & Casero, P. 1994b. Piggyback basin development and thrust belt evolution: structural and paleostress analyses of Plio–Quaternary basins in the Southern Apennines. *J. Struct. Geol.* **16**, 159–173.
Iorio, M. & Nardi, G. 1988. Studi paleomagnetici su rocce Mesozoiche dell Matese Occidentale. In: *L'Appennino Campano-lucano nel quadro geologico dell'Italia Meridionale*. Atti del 74° Congresso. *Soc. geol. ital.* Sorrento, 13–17 settembre 1988 (edited by De Frede). Napoli, 343–345.
Ippolito, F., Ortolani, F. & Russo, M. 1973. Struttura marginale Tirrenica dell'Appenino Campano. Reinterpretazioni di dati di antiche richerche di idrocarburi. *Mem. Soc. geol. ital.* **12**, 227–250.
Julien, Ph. & Cornet, F. H. 1987. Stress determinations from aftershocks of the Campania–Lucania earthquake of November 23, 1980. *Annal. Geophys.* **5B**, 289–300.
Kasten, K. A., Mascle, J. *et al.* 1990. Proc. ODP, Sci. Results, 107, College Station TX (Ocean Drilling Program).
Knott, S. D. & Turco, E. 1991. Late Cenozoic kinematics of the Calabrian arc, Southern Italy. *Tectonics* **10**, 1164–1172.
Kruse, S. E. & Royden, L. H. 1994. Bending and unbending of an elastic lithosphere: the Cenozoic history of the Apennine and Dinaride foredeep basins. *Tectonics* **13**, 278–302.
Malinverno, A. & Ryan, W. B. F. 1986. Extension of the Tyrrhenian Sea and shortening in the Apennines as result of a migration driven by sinking lithosphere. *Tectonics* **5**, 227–245.
McKenzie, D. P. 1969. The relation between fault plane solutions for earthquakes and the directions of the principal stresses. *Bull. seism. Soc. Am.* **59**, 591–601.
Mercier, J. L. & Carey-Gailhardis, E. 1989. Regional state of stress and characteristic fault kinematic instabilities shown by aftershock sequences: the aftershock sequences of the 1978 Thessaloniki (Greece) and 1980 Campania–Lucania (Italia) earthquakes as example. *Earth Planet Sci. Lett.* **92**, 247–264.
Mostardini, F. & Merlini, S. 1988. Appennino Centro-Meridionale: sezioni Geologiche e proposta di modello strutturale. *Mem. Soc. geol. ital.* **35**, 1986/1988, 177–202.
Moussat, E. 1983. Evolution de la Mer Tyrrhénienne Centrale et Orientale et de ses marges septentrionales en relation avec la néotectonique dans l'Arc Calabrais. Unpublished Ph.D. thesis, Université P. et M. Curie, Paris.